# A Printed U-Shaped Coplanar Waveguide Fed UWB Antenna for GPR Applications

Mohammed Guerroui<sup>1</sup>, Abdelhalim Chaabane<sup>1</sup>, Samir Ikni<sup>1</sup>, Ahcene Boualleg<sup>1</sup>, Nassima Guebgoub<sup>1</sup>, and Omar Mahri<sup>1</sup>

<sup>1</sup>Laboratoire des Télécommunications-LT, Département d'Electronique et Télécommunications, Faculté des Sciences et de la Technologie, Université 8 Mai 1945 Guelma, BP 401, Guelma 24000, Algeria.

Corresponding author: Mohammed Guerroui (e-mail: guerroui.mohammed@univ-guelma.dz).

**ABSTRACT** A printed U-shaped coplanar waveguide fed (CPW) ultra-wideband (UWB) antenna is designed, fabricated, and measured in this paper for ground penetrating (GPR) applications. Some cutoffs were introduced into different parts of the antenna to improve the working bandwidth. The antenna was printed on the FR4-epoxy substrate in a compact size of  $0.259\lambda_0 \times 0.309\lambda_0 \times 0.015\lambda_0$  at 3 GHz. The calculated results were validated by realizing and measuring a prototype. Experimental demonstrations were done using the R&S®ZNB Vector Network Analyzer, which indicates that the working bandwidth extends from 3.09 GHz to 11.07 GHz (112.71%). Additionally, the radiation patterns of the antenna were measured in an isolated anechoic chamber, which shows that the proposed antenna has omnidirectional radiation patterns. Moreover, acceptable antenna gain values ranging between 1.74 and 7.04 dBi and high values of radiation efficiency of more than 80% were achieved over the whole working bandwidth. Besides, the antenna presents a stable group delay with a linear phase of  $S_{21}$  through the UWB frequency band. To prove the efficiency of the fabricated antenna for GPR applications, the operation of the antenna was experimentally tested in a sandy soil box. The obtained results show that the proposed antenna could be a good candidate for GPR applications.

**INDEX TERMS** Coplanar Waveguide (CPW), Ground Penetrating Radar (GPR) Applications, Ultra-Wideband (UWB) Antenna, Voltage standing wave ratio (VSWR).

## I. INTRODUCTION

Ground penetrating radar (GPR) is a non-destructive testing system that exploits electromagnetic waves in a bandwidth extending between 0.1 GHz and 15 GHz for different civilian and military applications, such as detecting buried objects, scanning sub-surfaces, archaeological surveys, identification of hidden landmines, detecting voids in different materials like reinforced concrete, marble, wood, and detecting moisture in sandy soil. For all GPR systems, antennas are indispensable components that define their performance through transmitting and receiving electromagnetic waves. Furthermore, to provide the desired resolution and penetration depths, GPR systems require antennas with specific characteristics such as wide bandwidth with high radiation efficiency (> 70%), stable gain, linear phase of coefficient transmission, and non-varying group delay (<2 ns). An ultra-wideband (UWB) antenna is suitable for the capability of penetration at various depths. Accordingly, UWB antennas have recently received a large concentration to propose developed systems with efficacious antennas [1-12]. In this context, different GPR antennas have been presented in recent literature, such as those presented in [13-22]. In [13-14], a leaf-shaped antenna having a large size of 38.31 mm× 34.52 mm × 0.8 mm has been proposed for the penetration capability through three materials: sand, wood, and glass in [13], and through sandy soil in [14]. Likewise, in [15], the same antenna has been placed above two FSS layers for a sand penetration test. However, the main restraints are its large size of 44 mm × 44 mm × 24 mm and the used complicated periodic structures. The same FSS lavers have been used in [16] as a reflector below a circular disk-shaped UWB antenna. This antenna has a similar drawback of complexity and has a considerable size of about 44 mm × 44 mm × 34 mm. In [17], a tapered slot antenna has been proposed to penetrate the sandy soil. This design covers a narrow band ranging from 0.6 to 4 GHz and it has a voluminous size of 220 mm × 180 mm × 1.6 mm. A big bowtie antenna of dimensions has been presented in [18] for GPR application. It has large dimensions of about 107.7 mm × 68 mm × 0.8 mm and operates in a narrow band ranging between 0.98 and 4.5 GHz. A large size monopole UWB antenna coupled with single layer FSS has been proposed in [19] for subsurface scanning applications. An L-band horn antenna with a large dimension of 410 mm × 300 mm for landmine detection application has been proposed in [20]. In [21], a UWB rhombus-shaped antenna has been placed in touch contact with a limited and non-homogeneous solid mass of concrete that is constituted by mixing many



materials of different characteristics to test the capability of penetration. A circularly polarized UWB antenna with a question mark-shaped patch has been proposed for GPR application in [22]. Its penetration capability has not been tested in spite of its good characteristics. Most of these presented antennas have large bandwidth, but their high weight and bulky size limit their integration into GPR systems. In this work, a printed U-shaped CPW-fed UWB antenna is proposed for GPR applications. The simulation results and design analysis were conducted using the commercial software CST microwave studio<sup>TM</sup> [23]. A prototype of the designed antenna was fabricated and measured. Additionally, the operation of the fabricated prototype was tested on sandy soil to verify its capability of penetration.

### **II.ANTENNA DESCRIPTION AND RESULTS**

The front view of the designed U-shaped CPW-fed UWB antenna is schematically presented in fig. 1. The antenna design evolution is depicted in fig. 2. The length and the width of the initial rectangular patch were calculated using the two formulas (1) and (2) [24].

$$L_4 = \frac{\lambda_0}{2.\sqrt{\varepsilon_{eff}}} - 2.\Delta L_4 \tag{1}$$

$$2a = \frac{\lambda_0}{2} \left( \frac{\varepsilon_r + 1}{2} \right)^{-1/2} \tag{2}$$

Where  $\varepsilon_r$  and  $\lambda_0$  are the substrate permittivity and free space wavelength of the resonant frequency. The parameters  $\varepsilon_{eff}$  and  $\Delta L_4$  are the effective dielectric constant and the fringing field length, respectively, which were calculated using the formulas (3) and (4), respectively.

$$\varepsilon_{eff} = \frac{\varepsilon_r + 1}{2} + \frac{\varepsilon_r - 1}{2} \left( 1 + \frac{12.h}{2a} \right)^{-1/2} \tag{3}$$

$$\Delta L_4 = 0.412.h \left( \frac{\varepsilon_{eff} + 0.3}{\varepsilon_{eff} - 0.258} \right) \cdot \frac{(2a/h) + 0.264}{(2a/h) + 0.813}$$
 (4)

Where *h* is the thickness of the substrate.

The antenna is printed on the front face of an epoxy-FR4 substrate with a relative permittivity of 4.4, a loss tangent of 0.025, and a thickness of 1.5 mm. The total size of the designed antenna is  $0.259\lambda_0 \times 0.309\lambda_0 \times 0.015\lambda_0$  at 3 GHz. The antenna's radiator is a U-shaped connected to a CPW 50-ohm transmission line. Two symmetrically P-shaped structures were generated by cutting metal from the upper ground plane. This cut allows resonance frequencies to appear in the lower band of the UWB. Moreover, a split ring is introduced on the CPW-feed line to extend the higher band of the impedance bandwidth. The physical dimensions of the proposed antenna were set as follows: W = 25.2 mm,  $W_1 = 10.6$  mm,  $W_2 = 3.4$  mm,  $W_3 = 1.2$  mm,  $W_4 = 0.96$  mm,  $U_3 = 10.7$  mm,  $U_4 = 1$ 

R = 1.5 mm, r = 1.2 mm, a = 6.45 mm, b = 4 mm, c = 7 mm, d = 12 mm, g = 0.3 mm.

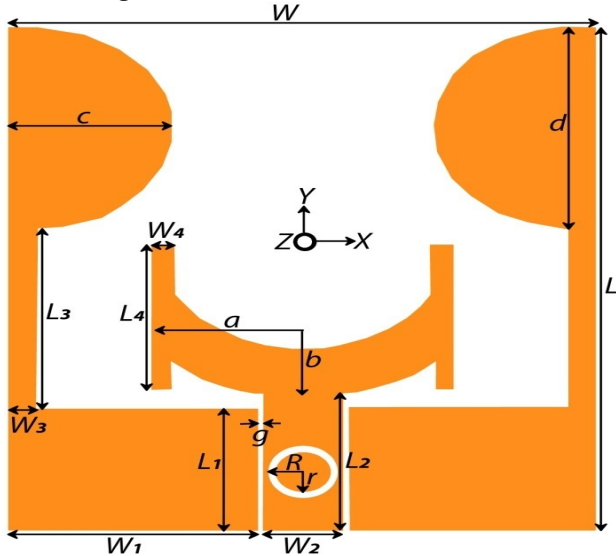


FIGURE 1. Front view and dimensions of the U-shaped CPW-fed antenna.

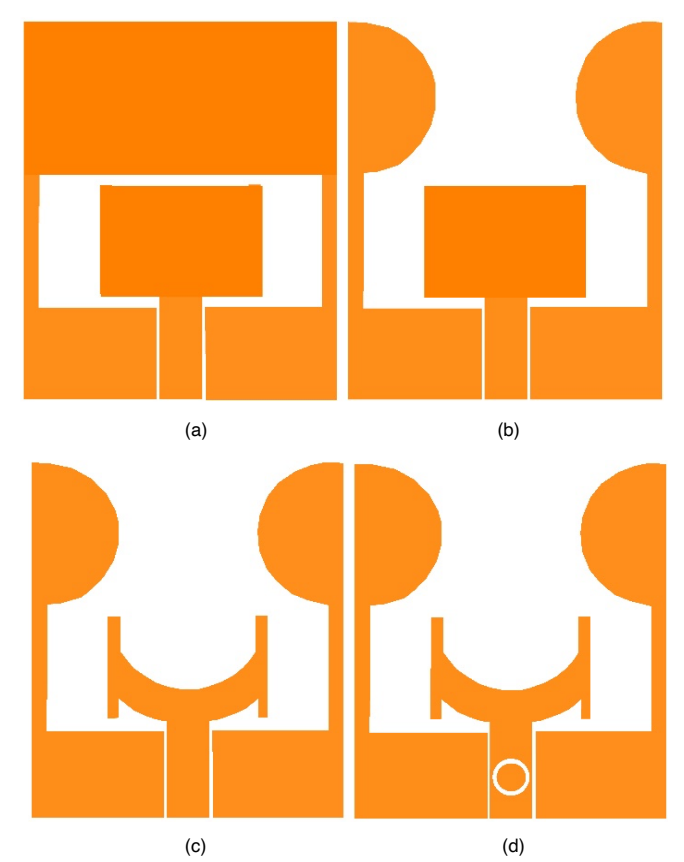


FIGURE 2. Antenna geometry evolution during the design stages, (a) antenna 1, (b) antenna 2, (c) antenna 3, (d) antenna 4.

The initial concept of the antenna consisted of an ordinary rectangular radiating patch with CPW-fed. As shown in fig. 3, the bandwidth of antenna 1 does not cover the UWB spectrum. In antenna 2, the metal is removed from the upper

part of the ground plane to affect the length of the current path. However, the bandwidth of antenna 2 still does not cover efficiently the UWB spectrum. Finally, in antenna 3 and antenna 4, a good adaption was achieved between 2.68 GHz to 11.28 GHz by removing the metal from the upper and bottom sides of the radiating patch and by etching a split ring in the feed line. In addition, as a result of these cuts, a lighter weight can be obtained and reduced conductor losses can be attained which are most wanted from the miniaturization viewpoint. Furthermore, Fig. 4 (a, b) shows the real and imaginary impedances of the four structures. Compared to the initial antennas, the designed antenna shows good matching impedance over the whole UWB range with the real part varying around 50 Ohms while the imaginary part is around 0 Ohms. This means that the maximum power supplied to the antenna will be emitted.

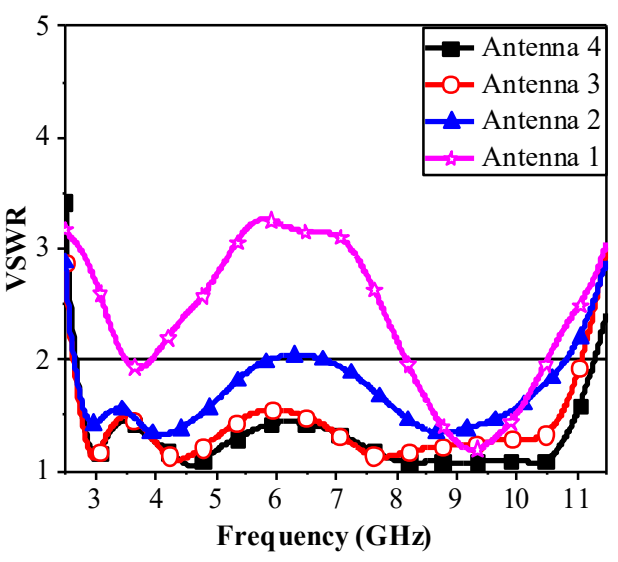
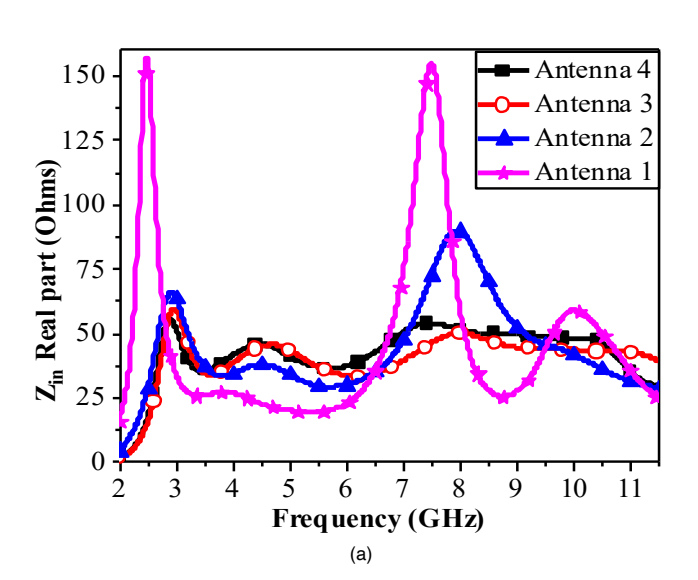
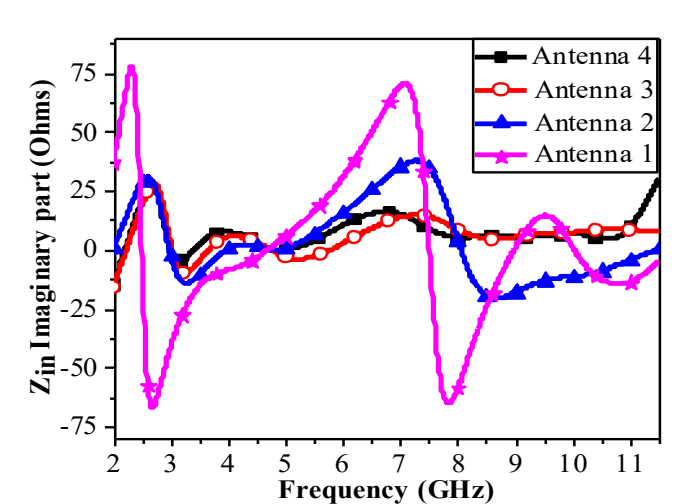
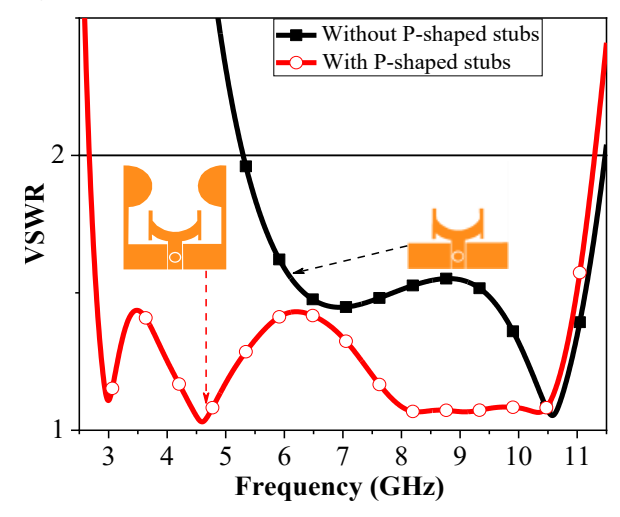


FIGURE 3. VSWR comparison of the designed antenna with those of the initial designs.





(b) FIGURE 4. The input impedance of the four designs. (a) real part, (b) imaginary part



**FIGURE 5.** Simulated VSWR performance of the proposed antenna with and without P-shaped stubs.

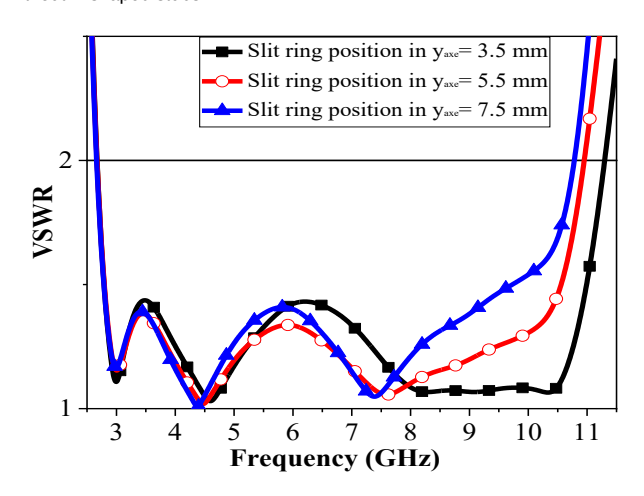




FIGURE 6. Influence of different positions of the split ring over the higher frequencies of the UWB.

Fig. 5 shows the influence of the two P-shaped stubs on the performance of the antenna at lower frequencies. The lower frequency of the antenna with the P-shaped stubs is 2.68 GHz while it becomes 5.3 GHz after removing the two P-shaped stubs. Thus, two P-shaped stubs have an essential role in enhancing the antenna impedance matching through the working UWB. The total length of each P-shaped stub which is 22.7 mm is approximately equivalent to about onequarter wavelength at the lower frequency band. That's why these stubs play an important role in generating resonances at lower frequencies and in enhancing the impedance matching at the lower frequency side. Moreover, the two P-shaped stubs increase the electrical size of the antenna which improves impedance matching at lower frequencies increasing the surface of the flowed current without enlarging the overall size. A better adaptation at higher frequencies and a wide impedance bandwidth are obtained by etching a split ring in the CPW-feed line. A parametric study has been carried out to find the optimum position of the split ring  $y_{axe}$ , along the CPW-feed line. The position of the split ring has been escalated by 2 mm starting from 3.5 mm to 7.5 mm. Fig. 6 indicates that the better position of the split ring along the CPW-feed line is at 3.5 mm.

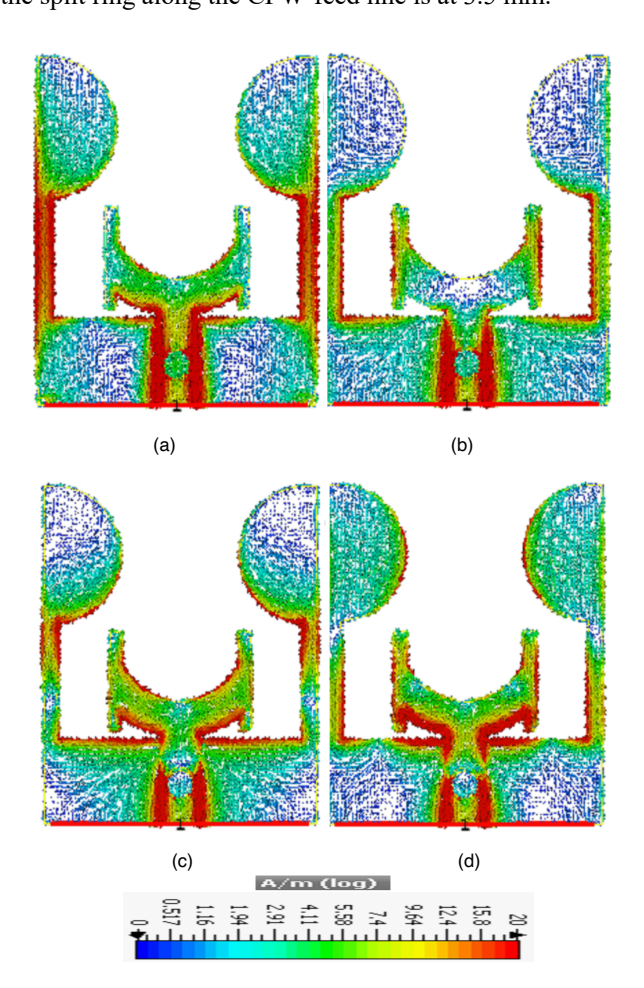


FIGURE 7. Current distribution on the antenna's surface at four frequencies (a) 3.6 GHz, (b) 5.77 GHz, (c) 8.33 GHz, and (d) 10.43 GHz.

Fig. 7 shows the current distribution on the different parts of the antenna at: 3.6 GHz, 5.77 GHz, 8.33 GHz, and 10.43 GHz, respectively. At 3.6 GHz, the maximum distribution appears on the two parallel parasitic strips where the length  $L_3$  of each one of them equals 10.7 mm, which is equivalent to about one-quarter wavelength at 3.6 GHz. That's why the two parallel parasitic strips play an important role in generating resonances at lower frequencies and in enhancing the impedance matching at the lower frequency side. Furthermore, at 5.77 GHz, the most significant current distribution concentrates on the gap between the transmission line and the ground plane and it is very weak on the two parallel parasitic strips. Moreover, a significant current distribution is shown on the radiating patch especially on its lower part at 8.33 GHz and 10.43 GHz. Thus, these stated parts have an essential role in the delimitation of the antenna's working bandwidth.

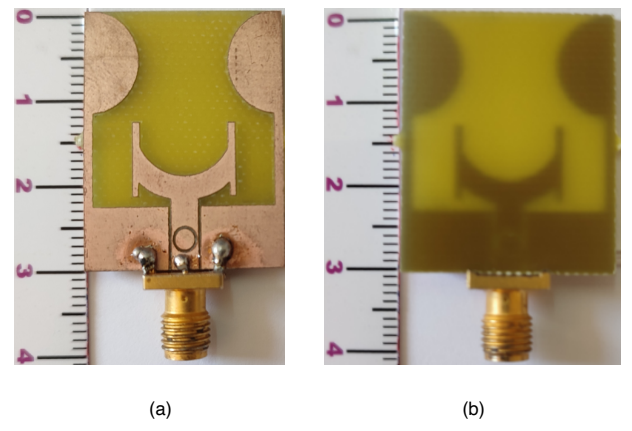


FIGURE 8. Fabricated prototype of the proposed U-shaped CPW-fed UWB antenna, (a) front view, (b) back view.

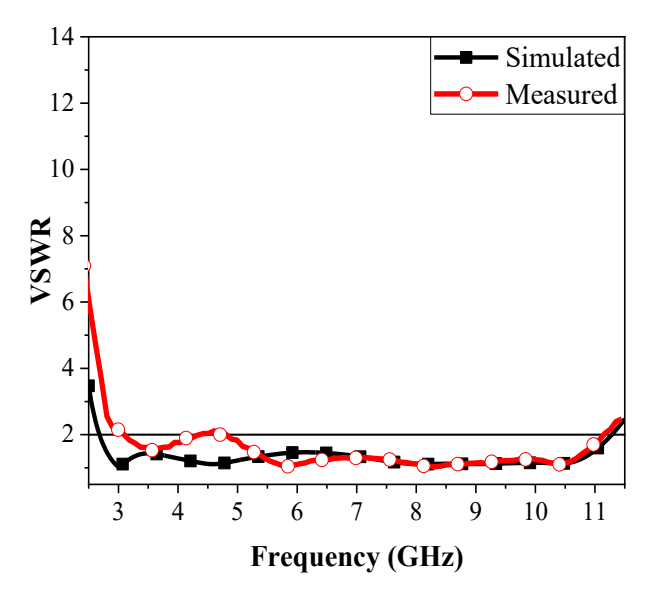
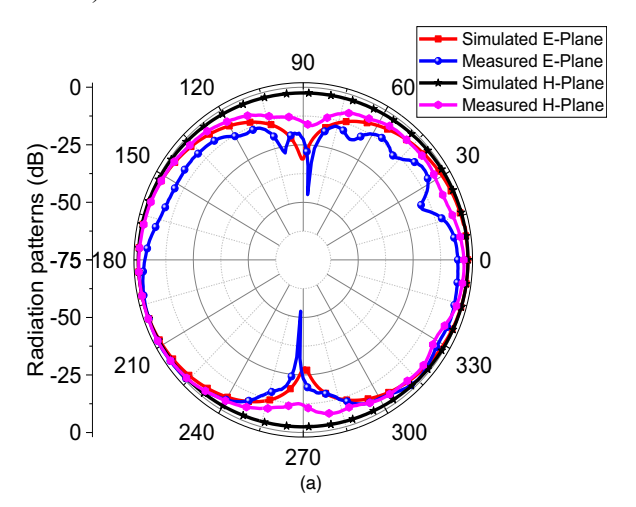


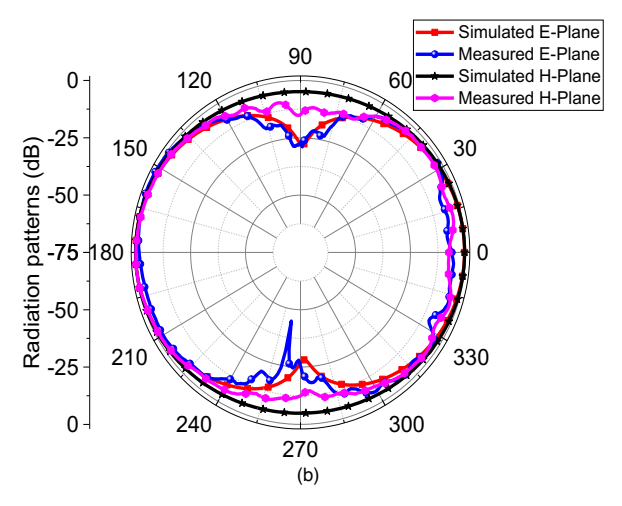
FIGURE 9. Measured and simulated VSWR of the proposed antenna.

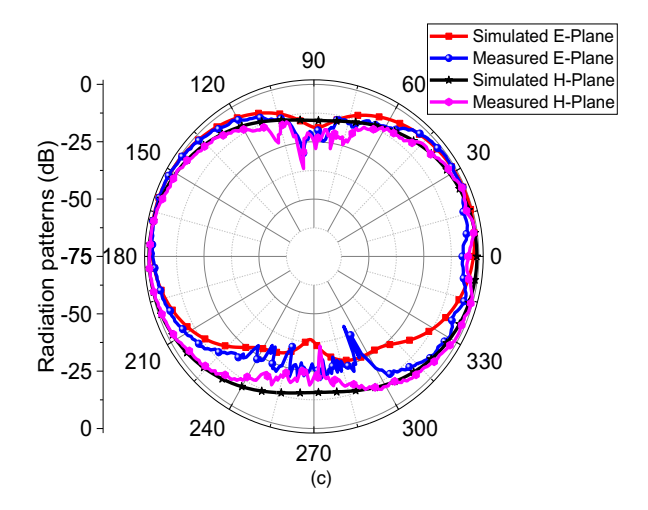


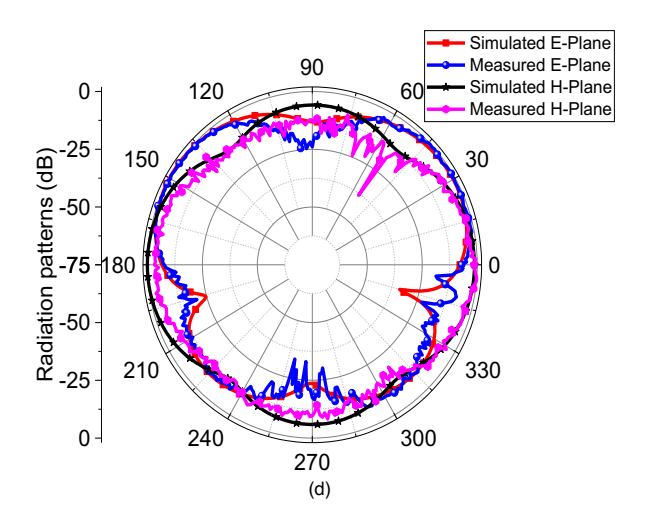
Fig. 8 represents a photograph of the realized prototype that was printed on the FR4-epoxy substrate by a laser printer (LPKF S103) with an entire size of  $0.259\lambda_0\times0.309\lambda_0\times0.015\lambda_0$  at 3 GHz. The VSWR of the fabricated prototype was measured by utilizing R&S®ZNB Vector Network Analyzer.

Fig. 9 represents the measured and simulated VSWR against the frequencies of the designed antenna. Good correlations between the simulation and the measurement were obtained and the UWB characteristic of the antenna is verified. The little mismatch, especially at lower frequencies, is mainly due to the measurement and fabrication errors and to the external electromagnetic disturbances which are not considered in the simulation. The calculated results of the bandwidth (VSWR < 2) show that the designed antenna operates from 2.68 GHz to 11.28 GHz (123.21%). Whereas the experimental results show that the fabricated antenna covers a broad bandwidth extending from 3.09 GHz to 11.07 GHz (112.71%) which is larger than the reserved UWB frequency band of 110% (3.1-10.6 GHz).









**FIGURE 10.** Simulated and Measured radiation patterns at four frequencies: (a) 3.6 GHz, (b) 5.77 GHz, (c) 8.33 GHz, (d) 10.43 GHz.

The antenna radiation patterns measurements of the fabricated prototype were measured in an isolated anechoic chamber. The experimental setup exploits two antennas which are the transmitting antenna (double ridged horn antenna-model AH-118 (1-18) GHz) and the antenna under test (the fabricated prototype) which is used as a receiving antenna. The simulated and measured values of radiation patterns in the xz-plane (H-plane) and the yz-plane (E-plane), at four frequencies (3.6 GHz, 5.77 GHz, 8.33 GHz, and 10.43 GHz), are reported in fig. 10. Similar to the results reported in [25,26], it is remarkable that the fabricated prototype has almost omnidirectional patterns in the H-plane and nearly bidirectional patterns in the E-plane. However, at higher frequencies, the far-field radiation patterns undergo inconsistency that is due to the excitation of higher order modes.

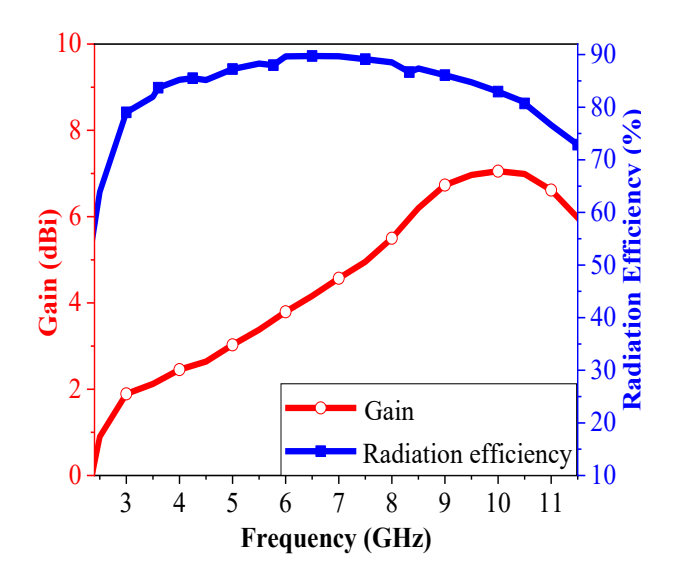


FIGURE 11. Gain and radiation efficiency achieved by the proposed antenna.

As can be observed in fig. 11, the simulated antenna gain and radiation efficiency performances against the frequency have significant values over almost the operating bandwidth; the antenna gain augments from 1.74 to 7.04 dBi with augmenting the frequency from 2.9 to 10.1 GHz. Moreover, the simulated antenna radiation efficiency is almost upper than 80% over the entire working bandwidth.

In order to verify the efficiency of the proposed antenna for GPR applications, an investigation into the time domain of group delay was carried out to check the distortion of the pulses between the transmitter and receiver antennas in two configurations: face-to-face and side-by-side as illustrated in fig. 12, where the distance between them was set to 30 cm. The two parameters group delay and the phase of  $S_{21}$  are particularly needed for radar and UWB applications.

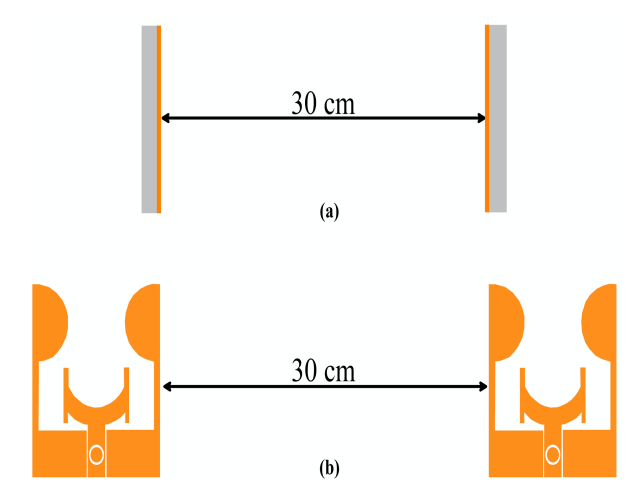


FIGURE 12. (a) Face-to-face configuration, (b) side-by-side configuration.

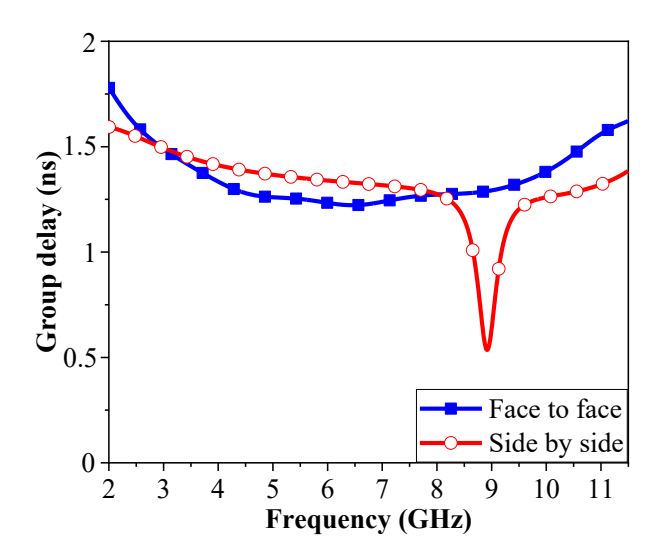


FIGURE 13. Simulated group delay in both configurations (Face-to-face and side-by-side).

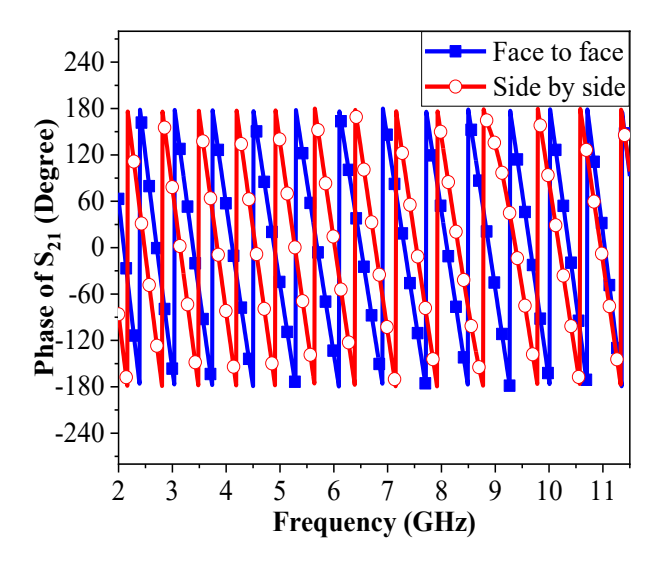


FIGURE 14. Simulated phase of S<sub>21</sub> in both configurations (Face-to-face and side-by-side).

Fig. 13 indicates that the variation of group delay in the face-to-face mode does not exceed 0.5 ns, while in the side-by-side mode it is less than 1 ns over the operational bandwidth. As shown in fig. 14, in both modes: face-to-face and side-by-side, the phase of  $S_{21}$  has linear variation over the working bandwidth. This is required for impulse radar systems, which need linear phase response and low dispersion.



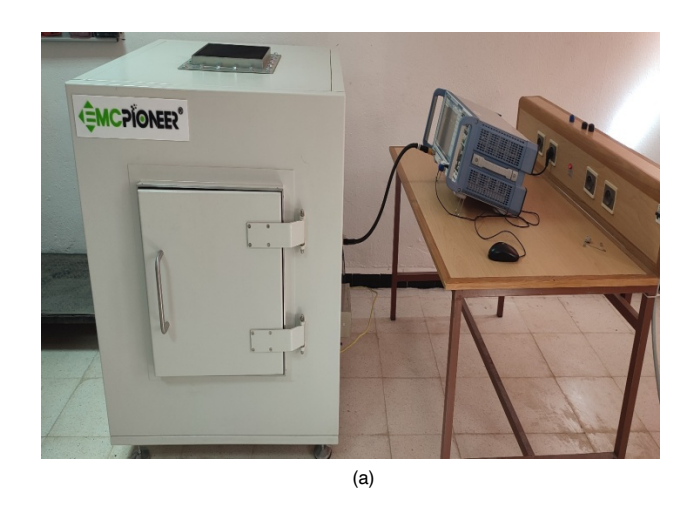
TABLE I. The designed antenna comparative analysis with other UWB antennas

Ref.	Substrate	Sizes (mm³)	Bandwidth (GHz)	Peak gain (dBi)
[27]	FR4	$\begin{array}{c} 0.36\lambda_0{\times}0.31\lambda_0 \\ \times 0.0083\lambda_0 \end{array}$	3.1-13.1	5
[28]	FR4	$0.402\lambda_0{\times}0.435\lambda_0{\times}0.\\0201\lambda_0$	4.02-10.7	3.54
[29]	FR4	$\begin{array}{c} 0.313\lambda_0{\times}0.313\lambda_0{\times}0\\ .0106\lambda_0 \end{array}$	2-9.5	3.5
[30]	FR4	$\begin{array}{c} 0.354\lambda_0{\times}0.326\lambda_0{\times}0\\ .0166\lambda_0 \end{array}$	3.32-20	7
[31]	FR4	$0.3\lambda_0{\times}0.208\lambda_0{\times}0.0\\13\lambda_0$	2.5-19.8	3.1
This work	FR4	$\begin{array}{c} 0.259\lambda_0\times0.309\lambda_0\\ \times0.015\lambda_0 \end{array}$	3.09-11.07	7

A comparison between the fabricated antenna and some other recent UWB planar antennas is shown in table 1. It is clear that the fabricated antenna is almost better in terms of peak gain and size than some other recent antennas.

# **III. GROUND PENETRATION TEST**

Firstly, the antenna was measured in an anechoic chamber. Then it is measured in front of a metal sheet. After that, the fabricated antenna was measured in touch with sandy soil. The measurement setup is constructed by a wooden box of size 400 mm × 300 mm× 350 mm filled by about 250 mm thick of dry sandy soil with a relative permittivity of 3. Fig. 15 presents the measurement setup used for the ground coupling GPR test. Fig. 16 indicates that by placing the fabricated antenna in touch with the sandy soil the antenna bandwidth is not significantly affected that still covers the UWB frequency band. A slight improvement at lower frequencies is observed due to the high penetration level characteristic of the low-frequency signals. It means that the fabricated antenna can radiate through the tested subsurface, and the excellent penetration capability is confirmed. Thus, we can conclude that the proposed antenna is suitable for GPR applications.





chamber, (b) in contact condition with the sandy soil box.

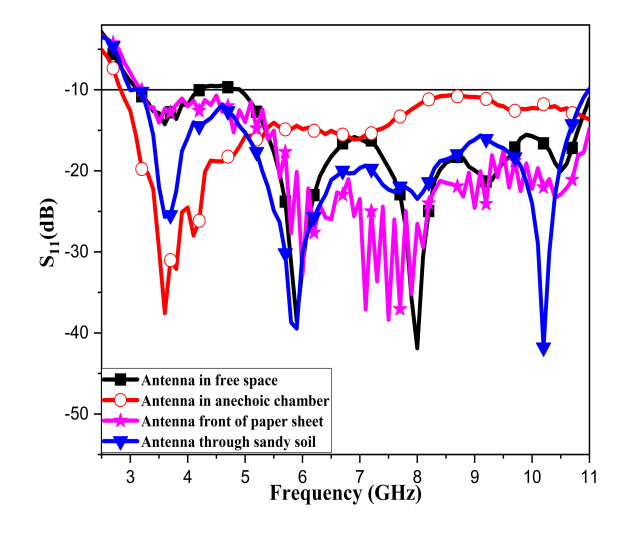


FIGURE 16. Comparison of the S<sub>11</sub> through different environments.



### IV. CONCLUSION

A printed U-shaped CPW-fed UWB antenna with good performance for GPR applications has been successfully designed, fabricated, and checked experimentally. The operating bandwidth has been extended by introducing a set of cuts on the radiating patch and the ground plane of the antenna. Experimental demonstrations performed with the R&S®ZNB Vector Network Analyzer show that the measured operating bandwidth extends from 3.09 GHz to 11.07 GHz (112.71%), covering the unlicensed UWB spectrum. The measurements established in an isolating anechoic chamber have shown that the fabricated antenna provides omnidirectional radiation patterns. Moreover, reasonable antenna gain and radiation efficiency have been calculated over the full working bandwidth. Besides a stable group delay with a linear phase of  $S_{21}$  have been attained. To verify the utility of the fabricated antenna for GPR applications, the antenna operation has been experimentally examined through a sandy soil box. A good capability of penetration is achieved. Accordingly, the proposed antenna could be an excellent candidate for GPR applications.

# **ACKNOWLEDGEMENT**

This work was supported by the Directorate General-for Scientific Research and Technological Development (DG-RSDT) of Algeria. The authors would like to thank Pr. Tayeb A. Denidni, INRS Canada, for his kind help for the antenna radiation patterns measurements.

# **REFERENCES**

- S. Liu, M. Li, H. Li, L. Yang, and X. Shi, "Cavity-backed bow-tie antenna with dielectric loading for ground-penetrating radar," IET Microwaves, Antenna & Propagation, vol. 14, no 2, pp. 153-157, November 2019.
- [2] D. N. Elsheakh, and E. A. Abdallah, "Compact ultra-wideband Vivaldi antenna for ground-penetrating radar detection applications," Microwave and Optical Technology Letters, vol. 61, no. 5, pp. 1268-1277, February 2019.
- [3] A. Raza, W. Lin, Y. Liu, A. B. Sharif, Y. Chen, and C. Ma, "A magnetic-loop based monopole antenna for GPR applications," Microwave and Optical Technology Letters, vol. 61, no. 4, pp. 1052-1057, December 2018.
- [4] A. Chaabane, and A. Babouri, "Dual band notched UWB MIMO for surfaces penetrating applications," Advanced Electromagnetics, vol. 8, no. 3, pp. 6-15, June 2019.
- [5] M. S. Hendevari, A. Pourzaid, and S. Nikmehr, "A novel ultrawideband monopole antenna for ground Penetrating Radar Applications," Microwave and Optical Technology Letters, vol. 60, no. 9, pp. 2252-2256, August 2018.
- [6] J. Ali, N. Abdullah, M. Y. Ismail, E. Mohd, and S. M. Shah, "Ultrawideband antenna design for GPR applications: A Review," International Journal of Advanced Computer Science and Applications (IJACSA), vol. 8, no. 7, August 2017.
- [7] M. Guerroui, A. Chaabane, and A. Boualleg, "Super UWB grooved and corrugated antenna for GPR application," Periodica Polytechnica Electrical Engineering and Computer Science, vol. 66, no. 1, pp. 31-37, January 2022.
- [8] S. Kundu, A. Chatterjee, S. K. Jana, and S. K. Parui, "A high gain dual notch compact UWB antenna with minimal dispersion for ground penetrating radar application," Radioengineering, vol. 27, no. 4, pp. 990–997, September 2018.
- [9] J. Ali, N. Abdullah, R. Yahya, I. Ullah, B. Das, and M. Jusoh, "Ultrawideband antenna development to enhance gain for surface

- penetrating radar," Wireless Personal Communication, vol. 115, no. 3, pp. 1821–1838, August 2020.
- [10] Y. Yang, J. Lu, R. Li, W. Zhao, and D. Yan, "Small-scale void-size determination in reinforced concrete using GPR," Advances in Civil Engineering, vol. 2020, pp. 1–11, June 2020.
- [11] W. Zatar, T. T. Nguyen, and H. Nguyen, "Predicting GPR signals from concrete structures using artificial intelligence-based method," Advances in Civil Engineering, vol. 2021, pp. 1–9, February 2021.
- [12] P. Prasad, S. Singh, and A. Kumar, "A wheel shaped compact uwb antenna for GPR applications," 2021 6th International Conference for Convergence in Technology (I2CT), April 2021.
- [13] S. Kundu, and S. K. Jana, "Leaf-shaped CPW-fed UWB antenna with triple notch band for ground Penetrating radar applications," Microwave and Optical Technology Letters, vol. 60, no. 4, pp. 930-936, March 2018.
- [14] S. Kundu, and S. K. Jana, "A leaf-shaped CPW-fed UWB antenna for ground Penetrating radar applications," Microwave and Optical Technology Letters, vol. 60, no. 4, pp. 941-945, March 2018.
- [15] S. Kundu, A. Chatterjee, S. K. Jana, and S. K. Parui, "Gain enhancement of a printed leaf shaped UWB antenna using dual FSS layers and experimental study for ground coupling GPR applications," Microwave and Optical Technology Letters, vol. 60, no. 6, pp. 1417–1423, April 2018.
- [16] S. Kundu, "Experimental study of CPW-fed printed UWB antenna with radiation improvement for ground coupling GPR application," Microwave and Optical Technology Letters, vol. 60, no. 10, pp. 2462–2467, September 2018.
- [17] A. Raza, W. Lin, Y. Chen, Z. Yanting, H. T. Chattha, and A. B. Sharif, "Wideband tapered slot antenna for applications in ground penetrating radar," Microwave and Optical Technology Letters, vol. 62, no. 7, pp. 2562–2568, March 2020.
- [18] M. Joula, V. Rafiei, and S. Karamzadeh, "High gain UWB bow-tie antenna design for ground penetrating radar application," Microwave and Optical Technology Letters, vol. 60, no. 10, pp. 2425–2429, September 2018.
- [19] S. Kundu, "A compact uniplanar ultra-wideband frequency selective surfaces for antenna gain improvement and ground penetrating radar application," International Journal of RF and Microwave computeraided engineering, vol. 30, no. 10, pp. e22363, August 2020.
- [20] A. H. Abdelgwad, and T. M. Said, "L-band horn antenna radiation enhancement for GPR applications by loading a wire medium," Microwave and Optical Technology Letters, vol. 59, no. 10, pp. 2558–2563, July 2017.
- [21] A. Chaabane, and M. Guerroui, "Printed UWB rhombus shaped antenna for GPR applications," Iranian Journal of Electrical and Electronic Engineering, vol. 17, no. 4, December 2021.
- [22] A. Chaabane, and M. Guerroui, "Circularly polarized UWB antenna with question mark shaped patch for GPR applications," Journal of Applied Research and Technology, vol. 20, no. 3, pp. 274–283, July 2022.
- [23] CST Microwave Studio, Computer Simulation Technology (CST) version 2016, Germany Available at: https://www.cst.com/Products/CSTMWS. 2016.
- [24] H. Abdi, J. Nourinia, and C. Ghobad, "Compact CPW-Fed Antenna for Enhanced UWB Applications," Advanced Electromagnetics, vol. 10, no. 1, pp.15-20, January 2021.
- [25] A. Chaabane, O. Mahri, D. Aissaoui, and N. Guebgoub, "Multiband Stepped Antenna for Wireless Communication Applications," Informacije MIDEM - Journal of Microelectronics, Electronic Components, and Materials, vol. 50, no. 4, pp. 275–284, January 2020.
- [26] B. Guenad, A. Chaabane, D. Aissaoui, A. Bouacha, and T. A. Denidni, "Compact cauliflower-shaped antenna for ultra-wideband applications," The Applied Computational Electromagnetics Society Journal (ACES), vol. 37, no. 1, pp. 68–77, May 2022.
- [27] S. Kundu and S. K. Jana, "A compact umbrella shaped UWB antenna for ground-coupling GPR applications," Microwave and Optical Technology Letters, vol. 60, no. 1, pp. 146–151, December 2017
- [28] M. Guerroui, A. Chaabane, and A. Boualleg, "A CPW-fed amended U-shaped monopole UWB antenna for surfaces penetrating applications," 2021 3rd International Congress on Human-Computer



- Interaction, Optimization and Robotic Applications (HORA), June 2021.
- [29] P. Khanna, A. Sharma, A. K. Singh, and A. Kumar, "A CPW-fed octagonal ring shaped ultra-wideband antenna for wireless applications," Advanced Electromagnetics, vol. 7, no. 3, pp. 87-92, August 2018.
- [30] D. Aissaoui, A. Chaabane, and A. Bouacha, "Compact super UWB elliptical antenna with corrugations for wireless communication
- systems," 2020 1st International Conference on Innovative Research in Applied Science, Engineering and Technology (IRASET), April 2020.
- [31] H. Abdi, J. Nourinia, and C. Ghobadi, "Compact enhanced CPW-fed antenna for UWB applications", Advanced Electromagnetics, vol. 10, no. 1, pp. 15–20, February 2021.